Chemical Engineering & Processing: Process Intensification 181 (2022) 109160

Contents lists available at ScienceDirect

Chemical Engineering and Processing - Process Intensification

journal homepage: www.elsevier.com/locate/cep

A comparative study on the decolorization of Tartrazine, Ponceau 4R, and Coomassie Brilliant Blue using persulfate and hydrogen peroxide based Advanced Oxidation Processes combined with Hydrodynamic Cavitation

Zahra Askarniya [a], Soroush Baradaran [b], Shirish H. Sonawane [c], Grzegorz Boczkaj [a,d,*]

[a] Department of Sanitary Engineering, Faculty of Civil and Environmental Engineering, Gdańsk University of Technology, 80-233, Gdańsk, 11/12 Narutowicza Str., Poland
[b] Department of Chemical Engineering, Iran University of Science and Technology (IUST), Tehran, Iran
[c] National Institute of Technology Warangal, Telangana State, India 506004
[d] EkoTech Center, Gdansk University of Technology, G.Narutowicza St. 11/12, 80-233 Gdansk, Poland

ARTICLE INFO

Keywords:
Cavitation
Persulfate
Hydrogen Peroxide
Wastewater Treatment
Oxidation
Radicals

ABSTRACT

Decolorization of Ponceau 4R, Tartrazine, and Coomassie Brilliant Blue (CBB) was studied using hybrid processes of hydrodynamic cavitation (HC) with potassium persulfate (KPS) and hydrogen peroxide (H_2O_2). The different properties of these dyes such as hydrophobicity, molecular structures, and molecular weights provided this opportunity to investigate the effects of these factors by comparing the decolorization values of the dyes. Treatment process was optimized in respect to cavitation number, HC inlet pressure, and the concentration of external oxidants. The application of dual oxidation system under cavitation conditions revealed a synergetic effect. Maximum decolorization values of 92.27%, 50.1%, and 42.3% were obtained applying this combined process for CBB, Tartrazine, and Ponceau 4R, respectively. The different values of decolorization of the dyes were explained based on their different properties. The kinetic study led to first order rate constants of 10^{-3} min^{-1}, $6.4*10^{-3}$ min^{-1}, $9.2*10^{-3}$ min^{-1}, and $4.16*10^{-2}$ min^{-1} using KPS, H_2O_2, HC, and HC-KPS-H_2O_2, respectively. A synergetic coefficient of 2.51 obtained by HC-KPS-H_2O_2 proved the effectiveness of this combined process. Analysis of cavitation yield efficiency showed an improvement of 98% for the HC-KPS-H_2O_2 combined process as compared to sole HC treatment process.

1. Introduction

Discharge of colored wastewater from a variety of sources such as textile and food industries into the environment has become a world-wide concern due to its undesirable effects on all organisms, including human beings and aquatic ones [1]. In fact, the pretreatment of this type of wastewater is one of the crucial challenges due to the toxicity and turbidity produced by synthetic dyes [2]. Dyes are classified in several categories including acidic and basic, reactive, disperse, and direct dyes [3]. The dyes possessing strong, complex, and penetrative color have high mineralization demand [4]. For the aim of treatment of colored effluent, it is essential to remove the color, which is obtained by the breakage of chromophore groups including azo (-N=N-), carbonyl (-C=O), nitro (-N=O), and quinoid groups [5]. Coomassie Brilliant Blue (CBB) is a non azo dye that is frequently used in textile industry and gel electrophoresis [6]. This dye is carcinogenic, mutagenic, teratogenic, and highly toxic to respiratory tract [7]. Tartrazine is an azo dye widely employed as an additive in textiles, cosmetics, and more frequently as a colorant in food industries. According to various studies, the dietary consumption of it can cause serious problems for humans such as anxiety, depression, vision and sleep disorders, asthma attack, atopic eczema, and anaphylactic shocks [8]. Ponceau 4R is another azo dye used as colorant in food industries, which can cause asthma and insomnia and may enhance children's hyperactivity and intolerance. Hence, in 2009, the European Food Safety Authority decreased the standard daily intake from 4.0 to 0.7 mg [9]. Safety of water comprising these dyes remains inconclusive; therefore, the best way to decrease risks is to develop more effective water and wastewater treatment methods.

Conventional treatment methods, including biodegradation are not

* Corresponding author: Department of Sanitary Engineering, Faculty of Civil and Environmental Engineering, Gdańsk University of Technology, 80 – 233 Gdansk, G. Narutowicza St. 11/12, Poland
E-mail address: grzegorz.boczkaj@pg.edu.pl (G. Boczkaj).

https://doi.org/10.1016/j.cep.2022.109160
Received 7 March 2022; Received in revised form 1 September 2022; Accepted 1 October 2022
Available online 7 October 2022

effective for many synthetic dyes. It follows from the complex molecular structure of these pollutants. Therefore, new efficient methods are required to be developed for the removal of these dyes [10]. HC is created by an instant drop of the local static pressure of a liquid flowing within a cavitating device such as an orifice plate or venturi tube, has shown its key role in the intensification of advanced oxidation processes (AOPs) employed for the treatment of textile wastewater [11–13]. Cavitational bubbles formed in the cavitation zone, as a result of pressure recovery in the downstream, collapse and generate high localized transient pressure and temperature of around 1000 atm and 10000 k, respectively, as well as high turbulence [14, 15]. These conditions can cause a pyrolytic decomposition of organic pollutants as well as water molecules and consequently the generation of hydroxyl radicals [16–18]. Hydroxyl radical is a strong oxidizing agent possessing an oxidation potential of 2.33 V, which can decompose a variety of dyes with a high reaction rate constant [19]. HC in combination with AOPs can lead to process intensification by enhancing the generation of reactive radicals attacking pollutants molecules and degrading them into less harmful compounds [20]. Furthermore, the combination of HC and AOPs can overcome mass transfer limitation because of the extreme conditions produced by the collapse of cavitation bubbles and microcirculation zones, resulting in the higher degradation rate of pollutants [21–23]. Therefore, these hybrid processes can be regarded as promising techniques for industrial wastewater treatment [20, 24]. Literature has proved the effectiveness of these combined processes such as the combination HC with Fenton [25], advanced Fenton [26], UV [27], and oxidants including O_2 [28], O_3 [27], H_2O_2 [29], and peroxone [30]. The researchers have thoroughly investigated an influence of HC on the decolorization of dyes. For instance, the effectiveness of HC with and without oxidizing agents for the decolorization of Rhodamine B [31–34], Rhodamine 6G [16], Methylene Blue [35], Brilliant Green [36], Brilliant Red [37], Reactive Red [38], Orange Acid-II [36], Direct Orange 46 [38], Orange G [39], Crystal Violet [40], Methyl Orange [41], Acid Red 88 [42], Reactive Red 120 [43], Reactive Orange 4 [44], Reactive Blue [45], and Congo Red [46] has been investigated.

Persulfate $(S_2O_8)^-$ is attracting attention because of its high solubility in water, appropriate utilization, stability at room temperature, cost effective, and easy availability. Another important advantage of persulfate is its wide operative pH [20, 47, 48]. The solubility of persulfate is around 5.3 g/100mL at 20°C, and this high solubility makes the utilization of persulfate feasible as an oxidant for wastewater treatment since it does not take a long time to dissolve in water, and it is also possible to use the high concentration of the oxidant, if it is needed [49]. Persulfate generates $SO_4^{\bullet-}$ under cavitation, which has longer half-life than $HO^{\bullet}$ [50]. Moreover, $SO_4^{\bullet-}$ are selective in nature and preferably reacts with electron donating groups such as hydroxyl (−OH), amino ($–NH_2$), alkoxy (–OR), π electrons of aromatic compounds, and unsaturated bonds. As a result, the combination of high oxidation potential, selectivity, and high stability of $SO_4^{\bullet-}$ makes this radical very efficient for wastewater treatment [51]. In contrast with ferrous sulphate combined with hydrogen peroxide in Fenton process for the production of $HO^{\bullet}$, persulfate does not generate any sludge. Additionally, it can be used in a wide range of pH but ferrous sulphate requires to be employed in acidic condition [47, 48]. Therefore, in comparison with ferrous sulfate, the application of persulfate eliminates the cost of remove of generated sludge and acidification. Activation of persulfate can occur through various methods in order to generate highly reactive sulfate radicals. For this purpose, UV, ferrous activation systems, photolysis, radiation, thermal activation as well as cavitation can be considered [51–53].

In a combined HC-AOP method, operating parameters such as cavitation number, inlet pressure, temperature, and reaction time along with type and dose of oxidizing agents as well as pH impact oxidation reaction yield. Intensity of the cavitation phenomenon resulted from bubble collapses can be attributed to the dimensionless cavitation number, that is dependent on differential pressure and flow rate [29, 54]. The efficacy of these combined processes and also the optimum amounts of additives extremely depend on the nature of pollutants, which necessitates the optimization of process parameters for each type of pollutants [55].

In the present work, HC, HC-KPS, and HC-KPS-H_2O_2 were investigated for the decolorization of CBB, Tartrazine, and Ponceau 4R. Although several studies have been devoted to the removal of dyes using hydrodynamic cavitation combined with persulfate, the synergy among persulfate and hydrogen peroxide has been rarely considered in the literature. Additionally, in our study, three dyes with different properties were selected to provide this opportunity to investigate the effect of molecular structure, hydrophobicity, and molecular weight through comparing the decolorization values of the dyes. In addition to the optimization studies, the yield efficiency of the combined processes was investigated to prove the effectiveness of them compared to individual ones. Moreover, the kinetic of processes was studied and the synergetic coefficient was calculated for the decolorization of the most decolorated dye to indicate the synergy among the processes. Since persulfate has a wide pH range of operation, it was preferred to perform this study without adjusting the pH of solution. This way no additional pH corrections before and after the treatment were needed.

2. Materials and Methods

2.1. Materials

Ponceau 4R, Tartrazine, and CBB were all provided from a viable domestic resource. Their main characteristics are described in Table 1, and their molecular structures are represented in Fig.1.

Hydrogen peroxide (50% %w/v) was purchased from LG chem (South Korea), and potassium persulfate (99%) was purchased from Samchun (South Korea).

2.2. Method

2.2.1. Experimental set-up

Experimental setup is presented in Fig.2.

A storage tank made of compact plastic with a volume of 10 liters equipped with a cooling coil was used for supply of treated wastewater. A centrifugal pump (PENTAX CBT600/00, 5.5 HP) was used to supply the intended pressure and flow rate of wastewater through the cavitation reactor. The research set-up was designed to regulate the flow and pressure via a bypass line and manual valves on each pipeline. A single hole orifice plate with conical entrance, a thickness of 5 mm, an inlet hole diameter of 4 mm, and a bevel angle of 45° was used as the cavitating device. In comparison with the straight hole orifice, the maximum velocity region is higher and the pressure recovery could be faster in the beveled one. Moreover, the beveled orifice affects the existence of dead zones that are influential for the chemical reactions. Cavitation reactor equipped with the orifice was made of Plexiglass to allow the visual observation of the HC phenomenon. The flow rate and pressure were measured by a flow meter and pressure gages, respectively. The mass of KPS was measured using a balance and then dissolved in 1 liter of water in a volumetric flask. Next, it was added to the main solution. The mass

Table 1
Characteristics of the dyes.

Dye	Chemical Formula	Molecular Weight	Water Solubility	Wavelength of visible light maximum absorbance (lambda max) [nm]
CBB	$C_{47}H_{50}N_3NaO_7S_2$	825.97	soluble	615
Tartrazine	$C_{16}H_9N_4Na_3O_9S_2$	534.36	20g/100mL	425
Ponceau 4R	$C_{20}H_{11}N_2Na_3O_{10}S_3$	604.46	soluble	518

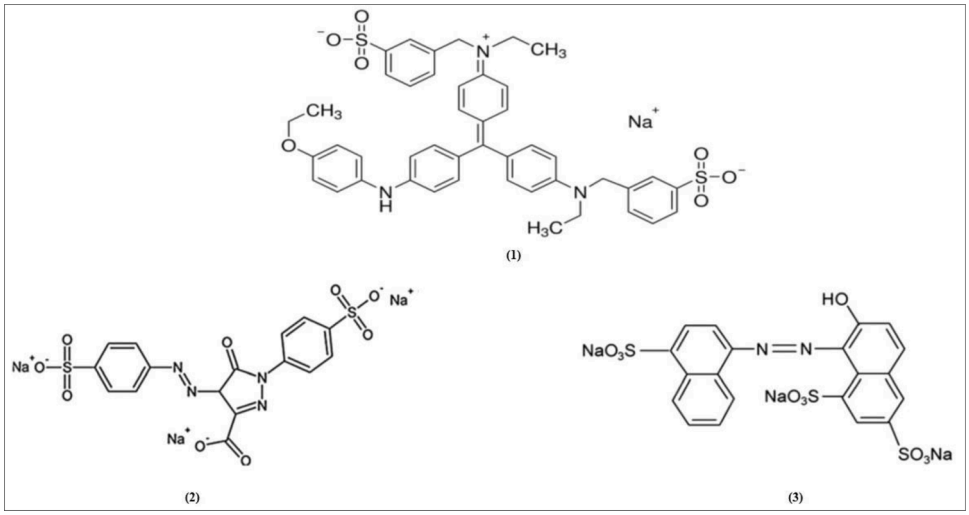

Fig. 1. Molecular structures of (1) CBB, (2) Tartrazine, (3) Ponceau 4R [56].

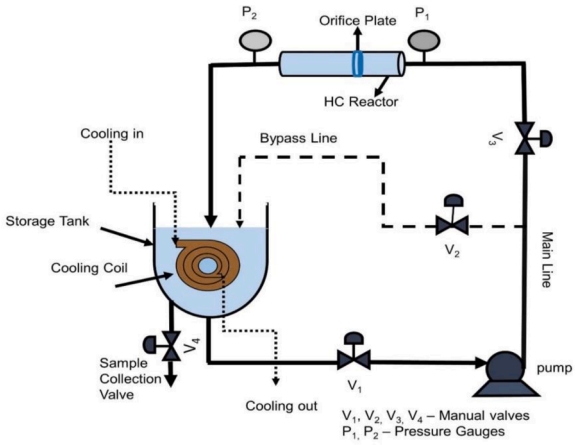

Fig. 2. HC experimental setup.

of H_2O_2 was converted to the volume using density and the equal volume was added to the solution using a pipette. The uncertainty of defined concentration of oxidants is negligible in respect to values magnitude as it relates to laboratory errors such as pipetting errors, calibration errors, and weighing errors, which influence the quality of measurement process. All the experiments were performed using an initial dyes concentration of 20 mg. L^{-1}, and the operating temperature was maintained at 30°C ±2.

2.2.2. Analytical method

UV–visible spectroscopic analysis was carried out by a UV-VIS Spectrophotometer (Hach DR/2010) at selected wavelength corresponding to a maximum on the UV-VIS spectrum of target pollutants to monitor the decolorization progress during the treatment process.

3. Results and Discussion

3.1. Effect of inlet pressure

Inlet pressure has a substantial impact on the effectiveness of hydrodynamic cavitation. Normally, a raise in inlet pressure up to an optimum value can increase the decolorization rate of pollutants. However, beyond this optimum amount, the removal of pollutants decreases [20, 57]. Cavitation number is a dimensionless number applied to present the extent of cavitation and it is calculated as following Eq.:

$$C_v = \frac{P_2 - P_v}{\frac{1}{2} \times \rho \times u^2} \quad (1)$$

C_v, P_2, P_v, ρ, and u express cavitation number, downstream recovered pressure (atmospheric pressure), vapor pressure, density, and the linear velocity of stream in the throat of a cavitating device. Cavitation number indicates the effects of inlet pressure which has direct influence on fluid velocity. In general, the inception of cavitation phenomenon and production of cavities occurs at $C_v \leq 1$ [38, 58].

Effect of inlet pressure on the decolorization of the dyes was evaluated through experiments applying different inlet pressures, and outcomes are shown in Table 2 and Fig.3.

Application of HC as sole process for the treatment resulted in 45.6% CBB decolorization, 16.36% Tartrazine decolorization, and 14.12% Ponceau 4R decolorization at an optimal inlet pressure of 6 bar. At an HC inlet pressure of 3 bar no decolorization was observed using sole HC, which can be an indication that the inception point of cavitation was probably at a pressure of 4 bar. As it can be observed increasing the inlet pressure from 4 bar to 6 bar resulted in a noticeable increase in the decolorization of all the dyes. Beyond this value, a slight decrease in the decolorization was noted, however, the values were basically different because of the different characteristics of the dyes. The enhanced decolorization achieved by increasing the HC inlet pressure resulted from several reasons. It may have facilitated the expansion of bubbles and intensified the collapse of them which led to extreme local temperatures and pressures and consequently, the intensification of the decolorization. Furthermore, inlet pressure affects cavitation zone, and increasing upstream pressure can lead to an increase in active volume used for oxidation reaction [59]. The drop observed in the decolorization at the pressures above 6 bar can be implied to the super cavitation phenomenon. This phenomenon can cause filled cavitation zone with a high number of cavities that usually contain the molecules of water vapor in the form of cavitation cloud. Despite an increase in cavities produced by an increase in pressure drop, cavity cloud is not able to collapse and create the extreme conditions that are responsible for decolorization [60, 61].

Table 2
. Operation parameters and cavitation number.

Inlet absolute pressure (bar)	Flow rate ($Lmin^{-1}$)	Cavitation Number (C_v)
4	15	0.47
5	19	0.31
6	22	0.23
7	26	0.16

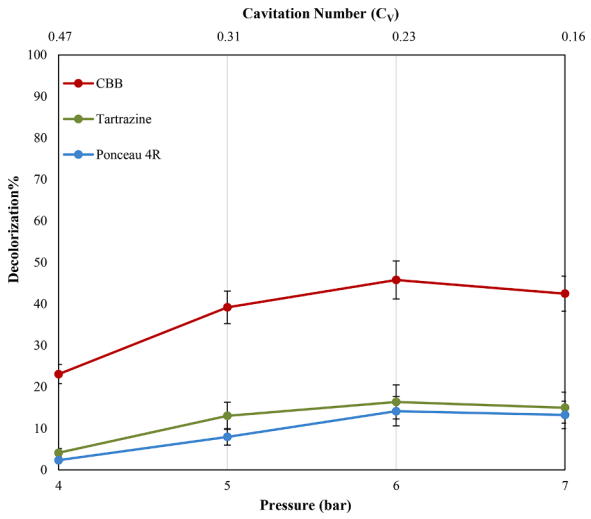

Fig. 3. Effect of HC inlet pressure on the decolorization of the dyes (reaction time = 60 min).

The trend can also be explained by Cavitation number (C_v). From the figure it is evident that the highest amount of decolorization occurred in a C_v of 0.23. It can be ascribed to the fact that low values of C_v led to the production of large quantity of cavitation bubbles and can intensify the effects of cavitation. While, it should be taken into accounts that too low values of C_v causes super cavitation and reduces the decolorization rate [62, 63].

Principally, the decolorization achieved by HC alone as a result of extremely high local pressures and temperatures created by the collapse of bubbles. This produced energy can lead to the decolorization by the pyrolytic decomposition of dyes molecules and water molecules. The decomposition of dyes molecules via HC extremely depends on the hydrophobicity of the dyes. Hydrophobicity is a characteristic which causes nonpolar molecules have a tendency to be distracted from water [64]. Hydrophobic molecules tend to move into the bubbles or place at the gas-liquid interfacial region, and the extreme energy created by these collapsing bubbles can result in the destruction of chromophore groups, on which the dye color is dependent, and therefore, results in the decolorization [59].

Using HC, the decolorization can also take place by typical AOP mechanism. The pyrolysis of water molecules results in formation of hydroxyl radicals according to Eq. (2).

$$H_2O \rightarrow {}^{\bullet}OH + {}^{\bullet}H \quad (2)$$

Hydroxyl radicals are strong oxidants that can react with dyes molecules and lead to the dissociation of chromophore groups and consequently, the decolorization of effluent.

3.2. Effect of KPS

In AOPs and cavitation-based AOPs, the concentration of oxidants extremely influences the production of reactive radicals. Hence, it is crucial to investigate this parameter to find the optimum amounts of oxidants, which increase the decolorization rate and decrease the cost of decontamination [65].

Persulfate ($S_2O_8^{2-}$) is a powerful oxidant, which can be regarded as a best option for the oxidation of water pollutants through the generation of reactive sulfate radicals [66]. The half-time of sulfate radicals is higher than hydroxyl radicals and its oxidation is based on the electron transfer mechanism. This radical prefers to react with electron donating groups like hydroxyl (-OH), alkoxy (-OR), and π electrons of aromatic rings [51]. Generated radicals can react with pollutants or be scavenged [67]. Reactions happening in the presence of Persulfate under HC are shown through the following reactions.

$$S_2O_8^{2-} + HC \rightarrow 2{}^{\bullet}SO_4^{-} \quad (3)$$

$${}^{\bullet}SO_4^{-} + {}^{\bullet}SO_4^{-} \rightarrow S_2O_8^{2-} \quad (4)$$

$${}^{\bullet}SO_4^{-} + S_2O_8^{2-} \rightarrow SO_4^{2-} + {}^{\bullet}S_2O_8^{-} \quad (5)$$

$$\bullet SO_4^{-} + H_2O \rightarrow SO_4^{2-} + {}^{\bullet}OH + H^{+} \quad (6)$$

In this study, the elimination of the pollutants was performed using Persulfate activated by HC due to the thermal effects of collapsing bubbles (Eq. 3) at different concentration values of persulfate. Although the same concentrations were used for each of the dyes, the rox, which is the molar ratio of oxidants to a pollutant, is different for each of them because of differences in their molecular weights. Obtained results are illustrated in Fig.4.

Accordingly, increasing KPS concentration up to 750 mg L^{-1} led to a rise in the decolorization of the dyes, while concentration exceeding this value slightly lowered the decolorization. It follows from self-scavenging mechanism due to the reaction of excess of KPS with formed radical species (Eq. 4 and 5).

At an optimum pressure of 6 bar, resulting in a C_v of 0.23, and a KPS concentration of 750 mg L^{-1}, 68.7% CBB decolorization, 27.3% Tartrazine decolorization, and 20.68% Ponceau 4R decolorization were observed using HC combined with KPS. Another important note which can be mentioned is the slight changes in Tartrazine and Ponceau 4R decolorization, indicating the low contribution of KPS loading to the decolorization of those dyes.

3.3. Effect of H_2O_2

H_2O_2 is described as a key source of reactive hydroxyl radicals possessing an oxidation potential of 2.33 V [68, 69]. An addition of H_2O_2 to the solution was expected to intensify the removal rate of pollutants because of generation of hydroxyl radicals depend on Eq. 7. The oxidation mechanism of hydroxyl radicals is based on both transfer of electrons and abstraction of hydrogen atoms [51]. Hydroxyl radicals can initiate the breakage of -C-N- in the structures of the dyes [13]. The reactions occurring using H_2O_2 under HC are indicated through the following Eqs.

$$H_2O_2 + HC \rightarrow 2\ OH^{\bullet} \quad (7)$$

$$H_2O_2 + OH^{\bullet} \rightarrow HO_2^{\bullet} + H_2O \quad (8)$$

$$HO_2^{\bullet} + HO_2^{\bullet} \rightarrow H_2O_2 + O_2 \quad (9)$$

$$OH^{\bullet} + O_2 \rightarrow HO_2^{\bullet} + O^{\bullet} \quad (10)$$

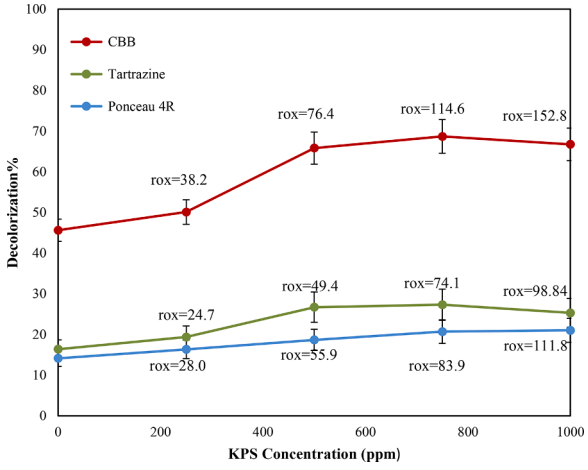

Fig. 4. Effect of KPS on the decolorization using HC-KPS (HC inlet pressure=6 bar, reaction time=60 min).

In addition, the synergetic effect of hydrogen peroxide with persulfate can enhance the decolorization rate by generating sulfate radicals and superoxide radicals through the reaction between persulfate and $HO_2^{\bullet}$, which is almost unreactive [70], according to Eq. 11 [65]. Superoxide radical is selective and mainly attacks -N=N- group, which can lead to the breakage of azo groups in the two azo dyes [13].

$$S_2O_8^{2-} + HO_2^{\bullet} \rightarrow {}^{\bullet}SO_4^{-} + SO_4^{2-} + H^{+} + O_2^{-\bullet} \quad (11)$$

Experiments were performed to investigate the influence of concentration of H_2O_2 on the decolorization of the dyes. The same concentrations of H_2O_2 were employed for the removal of the dyes, however the rox varied for each of the dyes. Outcomes of these experimentations are represented in Fig.5.

According to the results, increasing H_2O_2 up to the optimal amounts resulted in a surge in the decolorization of all the dyes, however, the optimum values depended on the type of the dyes. While the optimum values of concentration appeared at 500 mg L^{-1} for CBB and Tartrazine, in the case of Ponceau 4R, no significant change was observed in the concentration range from 250 mg L^{-1} to 750 mg L^{-1}. Beyond these optimum values, a decay in the decolorization was understood. The enhanced decolorization achieved by adding H_2O_2 to the solution can be attributed to activation of H_2O_2 molecules by HC and consequently the formation of hydroxyl radicals. The stability or reduction in the decolorization observed beyond optimum values results from scavenging influence of H_2O_2, i.e., the consumption of hydroxyl radicals by H_2O_2 based on Eq. 8.

The synergetic effect of the combined process was investigated for the dye with the highest value of decolorization. The decolorization of CBB was performed using individual HC, H_2O_2, and KPS as well as the combination of them and the decolorization was analyzed at a constant time interval of 10 min. The results of this investigation are demonstrated in Fig. 6.

First order rate constant of processes is calculated according to Eq. 12:

$$k = \frac{Ln\left(\frac{C_0}{C}\right)}{t} \quad (12)$$

Where k, t, C_0, and C stand for first order rate constant, reaction time, initial concentration, and concentration at a time of t, respectively.

The first order rate constants of the individual processes and the hybrid one were calculated and the results are observed in Fig. 7.

First order rate constant of 10^{-3} min^{-1}, $6.4*10^{-3}$ min^{-1}, $9.2*10^{-3}$ min^{-1}, and $4.16*10^{-2}$ min^{-1} were achieved using KPS, H_2O_2, HC, and HC-KPS-H_2O_2, respectively.

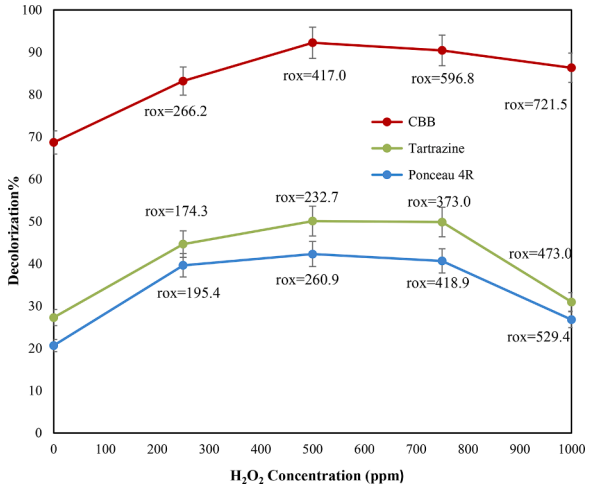

Fig. 5. Effect of H_2O_2 on the decolorization using HC-KPS-H_2O_2 (HC inlet pressure=6 bar, KPS concentration=750 mg L^{-1}, reaction time= 60 min).

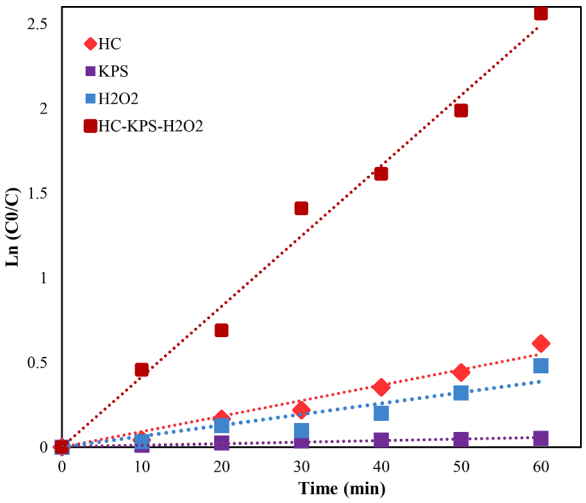

Fig. 6. Kinetics of decolorization of CBB.

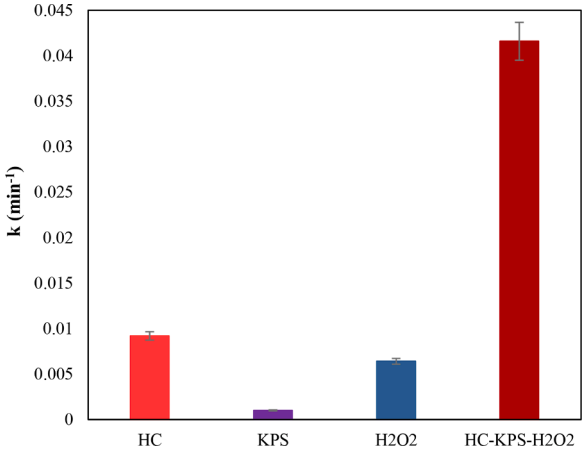

Fig. 7. First order rate constant of decolorization of CBB.

In order to indicate the synergy and effectiveness of the combined process, synergetic coefficient (SC) was calculated according to Eq. 13:

$$SC = \frac{k_{(HC-KPS-H2O2)}}{k_{HC} + k_{KPS} + k_{H2O2}} \quad (13)$$

A synergetic coefficient of 2.51 was obtained by the combined process of HC-KPS-H_2O_2, which can be an indication of process intensification achieved by HC.

Fig.8 compares the decolorization of the dyes achieved using hybrid as well as sole processes at a pressure of 6 bar for HC-based processes, a KPS concentration of 750 mg L^{-1}, and a H_2O_2 concentration of 500 mg L^{-1}. It is observed that CBB and Ponceau 4R had the highest and lowest percentages of the decolorization, respectively.

It is obvious that the combined process of HC-KPS-H_2O_2 was the most effective process for the decolorization of all the three investigated dyes, leading to 92.27% CBB decolorization, 50.1% Tartrazine decolorization, and 42.3% Ponceau 4R decolorization in 60 min.

The different values of decolorization of the dyes can be ascribed to differences in their properties such as hydrophobicity, molecular structures, and molecular weights [63]. It is observed that the decolorization of CBB was performed much more effectively than the decolorization of Tartrazine and Ponceau 4R, which are in azo dyes groups. It has been reported that dyes possessing more azo bonds are the most difficult to be decolorized through oxidation processes, and they might have a very small decolorization first order rate constant. In other words,

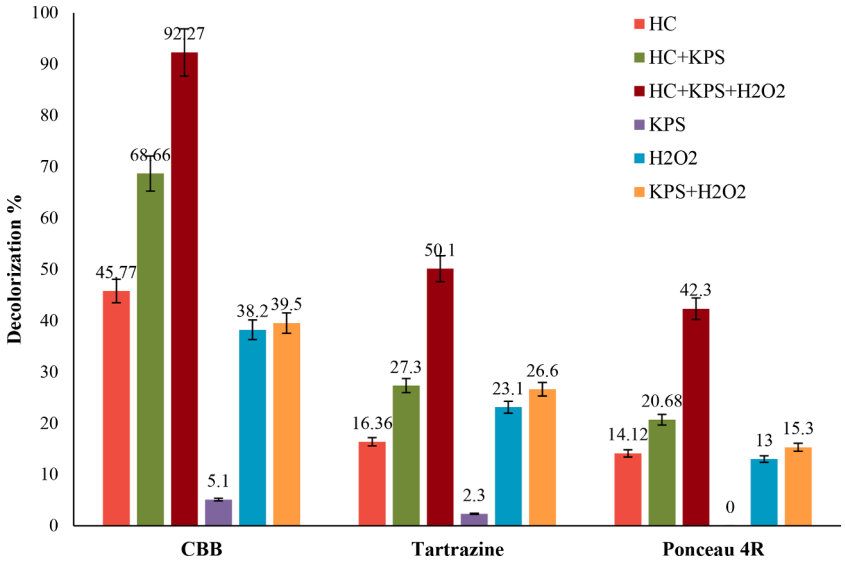

Fig. 8. Comparison of decolorization of the dyes (HC inlet pressure=6 bar, KPS concentration=750 mg L^{-1}, H_2O_2 concentration=500 mg L^{-1}, reaction time=60 min).

more azo dye bonds in the molecular structure of a dye can make it more resistant towards oxidation [71]; hence, it can be a reason for the lower decolorization of Tartrazine and Ponceau 4R compared to CBB. Differences in the degree of hydrophobicity of the dyes can be another reason explaining their different decolorization values. The presence of aromatic rings in the structures of molecules results in an increase in their hydrophobic property [72]. Hence, the higher value of decolorization of CBB can be attributed to the fact that it has a noticeable hydrophobic characteristic since it possesses 6 aromatic rings in its structure. Therefore, the molecules of this pollutant tend to exist within bubbles or in the interface area, where they can be decomposed directly by generated energy or by reacting with hydroxyl radicals produced through the decomposition of water molecules. Additionally, both KPS and H_2O_2 were activated by the energy generated through the collapse of bubbles; therefore, hydroxyl radicals and sulfate radicals were mainly in the vicinity of bubbles, where CBB molecules exist. Hence, the hydrophobicity of this dye made a remarkable contribution to its removal using HC, HC+KPS, and HC+KPS+H_2O_2. Ponceau 4R has a lower hydrophobic properties [72], and Tartrazine is almost categorized as a polar and hydrophilic dye [73]. Therefore, these two dyes mainly tended to be in the bulk of fluid, where the concentrations of reactive radicals were extremely lower than the inside of bubbles or in the interface of bubbles and fluid, which can be another reason for their low decolorization. Moreover, Higher molecular weights and more complex molecular structures result in lower reactivity of pollutants towards oxidants [63]. Therefore, among azo dyes, which lack strong hydrophobicity, the lower decolorization of Ponceau 4R compared to Tartrazine can be related to its higher molecular weight; nevertheless, the effect of this parameter is not significant since the difference between the decolorization values of these two dyes is not considerable. It can also be observed that the effect of presence of H_2O_2 on the decolorization of azo dyes is more evident than CBB. The addition of H_2O_2 led to an increase in the decolorization of CBB, Ponceau 4R, and Tartrazine by 34.39%, 83.52, and 104.54%, respectively. The extreme impact of the presence of H_2O_2 on the decolorization of the azo dyes can be related to the fact that superoxide radical generated through reaction 11 is a selective species and tends to mainly attack azo bonds. This reactive radical can be the main oxidative species responsible for the degradation azo dyes [13, 74].

3.4. Yield efficiency

The yield efficiency of combined processes is evaluated as per the Eq. (12) in order to determine the necessary energy for the decolorization of a precise amount of pollutants [29]:

$$\eta = \frac{\Delta C}{E_{pump}} \tag{14}$$

Where η, ΔC, and E_{pump} signify yield efficiency in mg kJ^{-1}, the amount of decolorization of a pollutant within certain time in mg, and the pump energy consumed at the same time in kJ. Fig.7 illustrates the results of the yield efficiency calculated for the decolorization of CBB, which has the higher decolorization using all studied processes.

Fig. 9

Yield efficiency values of 0.0063 mg kJ^{-1}, 0.0095 mg kJ^{-1}, and 0.0111 mg kJ^{-1} were achieved using HC, HC-KPS, and HC-H_2O_2 within 60 min, respectively. While a maximum yield efficiency of 0.0128 mg kJ^{-1} was achieved using the combined process of HC-KPS-H_2O_2 within 60 min. Using the combined process of HC-KPS-H_2O_2, the yield efficiency reached a high pick at the initial 10 min and then gradually dropped. This trend can be attributed to the fact that in the initial period of the experiment, the higher concentrations of the oxidants resulted in

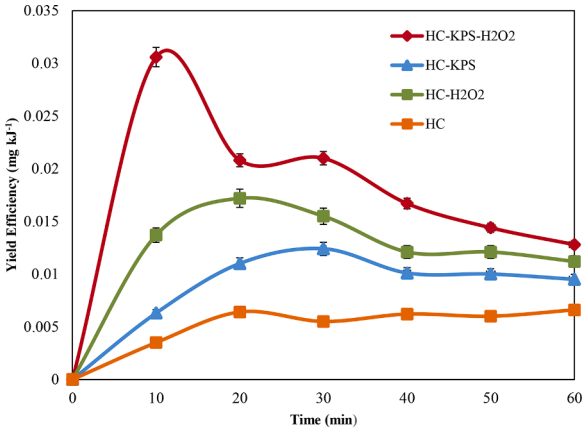

Fig. 9. Yield efficiency of decolorization of CBB via the various processes (HC inlet pressure=6 bar, KPS concentration=750 mg L^{-1}, H_2O_2 concentration=500 mg L^{-1}).

the higher number of reactive radicals which were responsible for the decolorization of the dye. Afterward, most of the oxidants were consumed while the pump was still working with the same energy, leading to a decrease in the yield efficiency [68]. Using sole HC, the yield efficiency touched a small peak at 20 min. It can be the result of high concentration of CBB in the initial minutes, which provides a high possibility of reaction between the dye and hydroxyl radicals generated by the pyrolysis of water molecules as well as a high chance of dye pollutant molecules being exposed to the energy generated by collapsing bubbles.

Moreover, the effect of the inlet pressures on the yield efficiency of HC treatment process was investigated and results are shown in Table 3.

As it is indicated in the Table 3, the highest yield efficiency values were attained at an optimal pressure of 6 bar for the decolorization all the investigated dyes using HC.

The cost of treatment for 92% decolorization of 1 L model effluent containing CBB using the combined process of HC-KPS-H_2O_2 was estimated. The cost of wastewater treatment using HC-based AOPs depends on a variety of factors such as the volume of effluent, time of treatment, type and concentration of pollutants, cost of oxidants, and cost of electricity [61]. In our study, the HC system worked at a power of 5.5 HP (4.1 Kw) and the reaction time was 60 min. The volume of medium fluid was 10 L, and the concentration of KPS and H_2O_2 were 750 mg L^{-1} and 500 mg L^{-1}, respectively. The price of electricity for industrial application is around 0.11 US dollars (USD) per kWh in Poland. The prices of hydrogen peroxide and potassium persulfate industrially used are in a range of 8-10 USD per L and 40-45 USD per kg. Therefore, the treatment cost for the decolorization of 1 L of model effluent containing 20 ppm CBB through HC-KPS-H_2O_2 is 0.08 USD (80 USD/1m^3), which can be regarded as an economical method based on the results achieved in previous studies [13, 75].

4. Conclusion

This study aimed at CBB, Tartrazine, and Ponceau 4R decolorization based on HC treatment process in combination with KPS and H_2O_2. The combined HC-KPS-H_2O_2 process was the most effective combination, and decolorizations of 92.27%, 50.1%, and 42.3% were attained by applying this combined process for CBB, Tartrazine, and Ponceau 4R, respectively. At the similar operating conditions, HC and HC-KPS resulted in 45.77% and 68.7% of CBB decolorization, 16.36% and 27.3% of Tartrazine decolorization, and 14.12% and 20.68% of Ponceau 4R decolorization, respectively. The decolorization of the dyes through HC process increased by an inlet pressure enhancement up to an optimum value. Beyond that, bubbles coalescence driving to super cavitation may have hindered the decolorization process. The values of decolorization for all the dyes via the HC-KPS and HC-KPS-H_2O_2 improved with increasing the concentration of the chemical agents up to maximum values. However, the optimum values are dependent upon the types of the dyes. Due to the hydrophobicity of CBB, the decolorization of this dye was by far easier than the two other dyes applying all HC-based processes. For CBB decolorization, first order rate constant of 10^{-3} min^{-1}, $6.4*10^{-3}$ min^{-1}, $9.2*10^{-3}$ min^{-1}, and $4.16*10^{-2}$ min^{-1} was achieved using KPS, H_2O_2, HC, and HC-KPS-H_2O_2, respectively, and a synergetic coefficient of 2.51 was obtained by the hybrid process. Furthermore, yield efficiency values of 0.0128 mg kJ^{-1}, 0.0111 mg kJ^{-1}, 0.0095 mg kJ^{-1}, and 0.0063 mg kJ^{-1}, were obtained via HC-KPS-H_2O_2, HC-H_2O_2, HC-KPS, and HC, respectively.

Declaration of competing Interest

The authors declare that they have no known competing financial interests or personal relationships that could have appeared to influence the work reported in this paper.

Table 3
Effect of inlet pressure on the yield efficiency of sole HC (reaction time= 60 min).

Pressure (bar)	CBB	Tartrazine	Ponceau 4R
	Yield Efficiency (mg kJ^{-1})		
4	0.0032	0.00057	0.00032
5	0.0054	0.0018	0.0011
6	0.0063	0.0023	0.002
7	0.0059	0.0021	0.0018

Data Availability

No data was used for the research described in the article.

References

[1] A.J. Sayyed, et al., Cellulose-based nanomaterials for water and wastewater treatments: A review, Journal of Environmental Chemical Engineering 9 (6) (2021), 106626.
[2] H. Deng, et al., Decolorization of Reactive Black 5 by Mesoporous Al2O3@ TiO2 Nanocomposites, Environmental Progress & Sustainable Energy 38 (s1) (2019) S230–S242.
[3] C.R. Holkar, et al., Biodegradation of reactive blue 19 with simultaneous electricity generation by the newly isolated electrogenic Klebsiella sp. C NCIM 5546 bacterium in a microbial fuel cell, International Biodeterioration & Biodegradation 133 (2018) 194–201.
[4] A.V. Mohod, et al., Process intensified removal of methyl violet 2B using modified cavity-bubbles oxidation reactor, Journal of environmental chemical engineering 6 (1) (2018) 574–582.
[5] C.R. Holkar, A.B. Pandit, D.V. Pinjari, Kinetics of biological decolorisation of anthraquinone based Reactive Blue 19 using an isolated strain of Enterobacter sp. F NCIM 5545, Bioresource technology 173 (2014) 342–351.
[6] M.P. Rayaroth, U.K. Aravind, C.T. Aravindakumar, Sonochemical degradation of Coomassie Brilliant Blue: Effect of frequency, power density, pH and various additives, Chemosphere 119 (2015) 848–855.
[7] M. Sun, et al., Thiourea-modified Fe3O4/graphene oxide nanocomposite as an efficient adsorbent for recycling Coomassie brilliant blue from aqueous solutions, Materials Chemistry and Physics 241 (2020), 122450.
[8] L. Khayyat, et al., Tartrazine induces structural and functional aberrations and genotoxic effects in vivo, PeerJ 5 (2017) e3041.
[9] A. Thiam, et al., Routes for the electrochemical degradation of the artificial food azo-colour Ponceau 4R by advanced oxidation processes, Applied Catalysis B: Environmental 180 (2016) 227–236.
[10] S. Rajoriya, et al., Treatment of textile dyeing industry effluent using hydrodynamic cavitation in combination with advanced oxidation reagents, Journal of Hazardous Materials 344 (2018) 1109–1115.
[11] S. Baradaran, M.T. Sadeghi, Intensification of diesel oxidative desulfurization via hydrodynamic cavitation, Ultrasonics sonochemistry 58 (2019), 104698.
[12] M. Zupanc, et al., Effects of cavitation on different microorganisms: The current understanding of the mechanisms taking place behind the phenomenon. A review and proposals for further research, Ultrasonics sonochemistry (2019).
[13] E. Cako, et al., Ultrafast degradation of brilliant cresyl blue under hydrodynamic cavitation based advanced oxidation processes (AOPs), Water Resources and Industry 24 (2020), 100134.
[14] S. Baradaran, M.T. Sadeghi, Desulfurization of Non-Hydrotreated Kerosene using Hydrodynamic Cavitation Assisted Oxidative Desulfurization (HCAOD) Process, Journal of Environmental Chemical Engineering (2020), 103832.
[15] S. Shirsath, et al., Ultrasound assisted synthesis of doped TiO2 nano-particles: characterization and comparison of effectiveness for photocatalytic oxidation of dyestuff effluent, Ultrasonics sonochemistry 20 (1) (2013) 277–286.
[16] S. Rajoriya, S. Bargole, V.K. Saharan, Degradation of a cationic dye (Rhodamine 6G) using hydrodynamic cavitation coupled with other oxidative agents: Reaction mechanism and pathway, Ultrasonics sonochemistry 34 (2017) 183–194.
[17] B. Bethi, et al., Novel hybrid system based on hydrodynamic cavitation for treatment of dye waste water: A first report on bench scale study, Journal of environmental chemical engineering 5 (2) (2017) 1874–1884.
[18] A.L. Prajapat, P.R. Gogate, Intensified depolymerization of aqueous polyacrylamide solution using combined processes based on hydrodynamic cavitation, ozone, ultraviolet light and hydrogen peroxide, Ultrasonics Sonochemistry 31 (2016) 371–382.
[19] C.R. Holkar, et al., A critical review on textile wastewater treatments: possible approaches, Journal of environmental management 182 (2016) 351–366.
[20] S. Baradaran, M.T. Sadeghi, Coomassie Brilliant Blue (CBB) degradation using hydrodynamic cavitation, hydrogen peroxide and activated persulfate (HC-H2O2-KPS) combined process, Chemical Engineering and Processing-Process Intensification 145 (2019), 107674.
[21] M. Torabi Angaji, R. Ghiaee, Decontamination of unsymmetrical dimethylhydrazine waste water by hydrodynamic cavitation-induced advanced Fenton process, Ultrason Sonochem 23 (2015) 257–265.

[22] K. Fedorov, X. Sun, G. Boczkaj, Combination of hydrodynamic cavitation and SR-AOPs for simultaneous degradation of BTEX in water, Chemical Engineering Journal 417 (2021), 128081.
[23] S. Raut-Jadhav, et al., Synergetic effect of combination of AOP's (hydrodynamic cavitation and H2O2) on the degradation of neonicotinoid class of insecticide, Journal of Hazardous Materials 261 (2013) 139–147.
[24] M. Gągol, et al., Effective degradation of sulfide ions and organic sulfides in cavitation-based advanced oxidation processes (AOPs), Ultrasonics sonochemistry 58 (2019), 104610.
[25] K. Roy, V.S. Moholkar, Sulfadiazine degradation using hybrid AOP of heterogeneous Fenton/persulfate system coupled with hydrodynamic cavitation, Chemical Engineering Journal 386 (2020), 121294.
[26] P.N. Patil, S.D. Bote, P.R. Gogate, Degradation of imidacloprid using combined advanced oxidation processes based on hydrodynamic cavitation, Ultrasonics sonochemistry 21 (5) (2014) 1770–1777.
[27] P. Thanekar, M. Panda, P.R. Gogate, Degradation of carbamazepine using hydrodynamic cavitation combined with advanced oxidation processes, Ultrasonics sonochemistry 40 (2018) 567–576.
[28] S.M. Joshi, P.R. Gogate, Intensification of industrial wastewater treatment using hydrodynamic cavitation combined with advanced oxidation at operating capacity of 70 L, Ultrasonics Sonochemistry 52 (2019) 375–381.
[29] H. Sayyaadi, Enhanced cavitation–oxidation process of non-VOC aqueous solution using hydrodynamic cavitation reactor, Chemical Engineering Journal 272 (2015) 79–91.
[30] G. Boczkaj, et al., Effective method of treatment of effluents from production of bitumens under basic pH conditions using hydrodynamic cavitation aided by external oxidants, Ultrasonics sonochemistry 40 (2018) 969–979.
[31] X. Wang, et al., Chemical effect of swirling jet-induced cavitation: degradation of rhodamine B in aqueous solution, Ultrason Sonochem 15 (4) (2008) 357–363.
[32] G. Mancuso, et al., Decolourization of Rhodamine B: A swirling jet-induced cavitation combined with NaOCl, Ultrason Sonochem 32 (2016) 18–30.
[33] X. Wang, et al., Degradation of rhodamine B in aqueous solution by using swirling jet-induced cavitation combined with H2O2, J Hazard Mater 169 (1-3) (2009) 486–491.
[34] K.P. Mishra, P.R. Gogate, Intensification of degradation of Rhodamine B using hydrodynamic cavitation in the presence of additives, Separation and Purification Technology 75 (3) (2010) 385–391.
[35] M.S. Kumar, S. Sonawane, A.B. Pandit, Degradation of methylene blue dye in aqueous solution using hydrodynamic cavitation based hybrid advanced oxidation processes, Chemical Engineering and Processing: Process Intensification 122 (2017) 288–295.
[36] P.R. Gogate, G.S. Bhosale, Comparison of effectiveness of acoustic and hydrodynamic cavitation in combined treatment schemes for degradation of dye wastewaters, Chemical Engineering and Processing: Process Intensification 71 (2013) 59–69.
[37] J. Wang, et al., Degradation of reactive brilliant red K-2BP in aqueous solution using swirling jet-induced cavitation combined with H2O2, Ultrason Sonochem 18 (2) (2011) 494–500.
[38] Y. Çalışkan, H.C. Yatmaz, N. Bektaş, Photocatalytic oxidation of high concentrated dye solutions enhanced by hydrodynamic cavitation in a pilot reactor, Process Safety and Environmental Protection 111 (2017) 428–438.
[39] M. Cai, et al., Decolorization of azo dyes Orange G using hydrodynamic cavitation coupled with heterogeneous Fenton process, Ultrasonics sonochemistry 28 (2016) 302–310.
[40] B. Bethi, et al., Investigation of TiO2 photocatalyst performance for decolorization in the presence of hydrodynamic cavitation as hybrid AOP, Ultrasonics sonochemistry 28 (2016) 150–160.
[41] P. Li, et al., Enhanced decolorization of methyl orange using zero-valent copper nanoparticles under assistance of hydrodynamic cavitation, Ultrasonics sonochemistry 22 (2015) 132–138.
[42] V.K. Saharan, et al., Hydrodynamic cavitation as an advanced oxidation technique for the degradation of acid red 88 dye, Industrial & Engineering Chemistry Research 51 (4) (2011) 1981–1989.
[43] V.K. Saharan, M.P. Badve, A.B. Pandit, Degradation of Reactive Red 120 dye using hydrodynamic cavitation, Chemical Engineering Journal 178 (2011) 100–107.
[44] M.M. Gore, et al., Degradation of reactive orange 4 dye using hydrodynamic cavitation based hybrid techniques, Ultrasonics sonochemistry 21 (3) (2014) 1075–1082.
[45] S. Rajoriya, S. Bargole, V.K. Saharan, Degradation of reactive blue 13 using hydrodynamic cavitation: Effect of geometrical parameters and different oxidizing additives, Ultrason Sonochem 37 (2017) 192–202.
[46] Z. Askarniya, M.-T. Sadeghi, S. Baradaran, Decolorization of Congo red via hydrodynamic cavitation in combination with Fenton's reagent, Chemical Engineering and Processing - Process Intensification 150 (2020), 107874.
[47] F. Ji, et al., Efficient performance of porous Fe2O3 in heterogeneous activation of peroxymonosulfate for decolorization of Rhodamine B, Chemical engineering journal 231 (2013) 434–440.
[48] J. Lee, U. Von Gunten, J.-H. Kim, Persulfate-based advanced oxidation: critical assessment of opportunities and roadblocks, Environmental science & technology 54 (6) (2020) 3064–3081.
[49] J. Kronholm, M.-L. Riekkola, Potassium persulfate as oxidant in pressurized hot water, Environmental science & technology 33 (12) (1999) 2095–2099.
[50] W.-D. Oh, Z. Dong, T.-T. Lim, Generation of sulfate radical through heterogeneous catalysis for organic contaminants removal: current development, challenges and prospects, Applied Catalysis B: Environmental 194 (2016) 169–201.
[51] K. Fedorov, et al., Ultrasound-assisted heterogeneous activation of persulfate and peroxymonosulfate by asphaltenes for the degradation of BTEX in water, Journal of Hazardous Materials 397 (2020), 122804.
[52] Y.-q. Gao, et al., Ultraviolet (UV) light-activated persulfate oxidation of sulfamethazine in water, Chemical Engineering Journal 195 (2012) 248–253.
[53] Z.-H. Diao, et al., Simultaneous removal of Cr (VI) and phenol by persulfate activated with bentonite-supported nanoscale zero-valent iron: reactivity and mechanism, Journal of hazardous materials 316 (2016) 186–193.
[54] A. Šarc, et al., The issue of cavitation number value in studies of water treatment by hydrodynamic cavitation, Ultrasonics Sonochemistry 34 (2017) 51–59.
[55] P.R. Gogate, P.N. Patil, Combined treatment technology based on synergism between hydrodynamic cavitation and advanced oxidation processes, Ultrasonics sonochemistry 25 (2015) 60–69.
[56] D.F. Oliveira, et al., Evaluating the effectiveness of photocatalysts based on titanium dioxide in the degradation of the dye Ponceau 4R, Dyes and Pigments 92 (1) (2012) 563–572.
[57] P. Thanekar, P.R. Gogate, Combined hydrodynamic cavitation based processes as an efficient treatment option for real industrial effluent, Ultrasonics sonochemistry 53 (2019) 202–213.
[58] P.S. Kumar, M.S. Kumar, A. Pandit, Experimental quantification of chemical effects of hydrodynamic cavitation, Chemical Engineering Science 55 (9) (2000) 1633–1639.
[59] S. Baradaran, M.T. Sadeghi, Coomassie Brilliant Blue (CBB) degradation using hydrodynamic cavitation, hydrogen peroxide and activated persulfate (HC-H2O2-KPS) combined process, Chemical Engineering and Processing - Process Intensification 145 (2019), 107674.
[60] Z. Abbas-Shiroodi, M.-T. Sadeghi, S. Baradaran, Design and Optimization of a Cavitating device for Congo Red Decolorization: Experimental Investigation and CFD Simulation, Ultrasonics Sonochemistry (2020), 105386.
[61] M. Gągol, A. Przyjazny, G. Boczkaj, Wastewater treatment by means of advanced oxidation processes based on cavitation–a review, Chemical Engineering Journal 338 (2018) 599–627.
[62] A.P. Bhat, P.R. Gogate, Cavitation-based pre-treatment of wastewater and waste sludge for improvement in the performance of biological processes: A review, Journal of Environmental Chemical Engineering 9 (2) (2021), 104743.
[63] A.J. Barik, P.R. Gogate, Hybrid treatment strategies for 2, 4, 6-trichlorophenol degradation based on combination of hydrodynamic cavitation and AOPs, Ultrasonics sonochemistry 40 (2018) 383–394.
[64] Y. Cao, J. Zhao, Y.L. Xiong, Coomassie Brilliant Blue-binding: a simple and effective method for the determination of water-insoluble protein surface hydrophobicity, Analytical Methods 8 (4) (2016) 790–795.
[65] M. Ahmadi, Hydrogen Peroxide/Zero Valent Iron/Persulfate Approach for Dye Degradation, Key Operating Parameter and Synergistic Effect, 2021.
[66] X.-R. Xu, X.-Z. Li, Degradation of azo dye Orange G in aqueous solutions by persulfate with ferrous ion, Separation and purification technology 72 (1) (2010) 105–111.
[67] J. Choi, et al., Hydrodynamic cavitation and activated persulfate oxidation for degradation of bisphenol A: Kinetics and mechanism, Chemical Engineering Journal 338 (2018) 323–332.
[68] Z. Askarniya, M.-T. Sadeghi, S. Baradaran, Decolorization of Congo red via hydrodynamic cavitation in combination with Fenton's reagent, Chemical Engineering and Processing-Process Intensification 150 (2020), 107874.
[69] Krumova, K. and G. Cosa, Overview of reactive oxygen species. 2016.
[70] P. Rao, E. Hayon, Redox potentials of free radicals. IV. Superoxide and hydroperoxy radicals. O2-and. HO2, The Journal of Physical Chemistry 79 (4) (1975) 397–402.
[71] H.-Y. Shu, M.-C. Chang, Decolorization effects of six azo dyes by O3, UV/O3 and UV/H2O2 processes, Dyes and pigments 65 (1) (2005) 25–31.
[72] G.M.D. Ferreira, et al., Adsorption of red azo dyes on multi-walled carbon nanotubes and activated carbon: A thermodynamic study, Colloids and Surfaces A: Physicochemical and Engineering Aspects 529 (2017) 531–540.
[73] B. Barry, G. Gray, Coacervation of alkyltrimethylammonium bromides by tartrazine, amaranth, carmoisine, and erythrosine, Journal of pharmaceutical sciences 63 (4) (1974) 548–559.
[74] D. Wang, et al., Effective degradation of Orange G and Rhodamine B by alkali-activated hydrogen peroxide: roles of HO2− and O2·−, Environmental Science and Pollution Research 26 (2) (2019) 1445–1454.
[75] M. Gągol, A. Przyjazny, G. Boczkaj, Highly effective degradation of selected groups of organic compounds by cavitation based AOPs under basic pH conditions, Ultrasonics sonochemistry 45 (2018) 257–266.